Thermodynamics with 2 + 1 + 1 Dynamical Quark Flavors

Stefan Krieg for the Wuppertal-Budapest Collaboration

Abstract We report on our calculation of the equation of state of Quantum Chromodynamics (QCD) from first principles, through simulations of Lattice QCD. We use an improved lattice action and $N_f = 2 + 1 + 1$ dynamical quark flavors and physical quark mass parameters. Now, we are in a position to present first results at $N_t = 12$.

1 Introduction

The aim of our project is to compute the charmed equation of state for Quantum Chromodynamics (for details, see [1]). We are using the lattice discretized version of Quantum Chromodynamics, called lattice QCD, which allows simulations of the theory through importance sampling methods. Our results are important input quantities for phenomenological calculations and are required to understand experiments aiming to generate a new state of matter, called Quark-Gluon-Plasma, such as the upcoming FAIR at GSI, Darmstadt.

Our simulations are performed using so-called staggered fermions. In the continuum limit, i.e. at vanishing lattice spacing a, one staggered Dirac operator implements four flavors of mass degenerate fermions. At finite lattice spacing, however, discretization effects induce an interaction between these would be flavors lifting the degeneracy. The "flavors" are, consequentially, renamed to "tastes", and the interactions are referred to as "taste-breaking" effects. Even though the tastes are not degenerate, in simulations one takes the fourth root of the staggered fermion determinant to implement a single flavor. This procedure is not proven to be correct—however, practical evidence suggests that is does not induce errors visible with present day statistics.

S. Krieg (✉)
Fachbereich C - Physik, Bergische Universität Wuppertal, 42119 Wuppertal, Germany

IAS, Jülich Supercomputing Centre, Forschungszentrum Juelich GmbH, 52425 Jülich, Germany
e-mail: krieg@uni-wuppertal.de

W.E. Nagel et al. (eds.), *High Performance Computing in Science and Engineering '15*, DOI 10.1007/978-3-319-24633-8_1

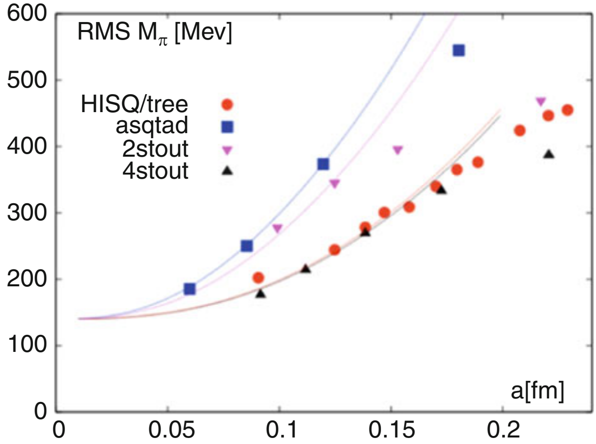

Fig. 1 RMS pion mass for different staggered fermion actions, in the continuum limit

Taste-breaking is most severely felt at low pion masses and large lattice spacing, as the pion sector is distorted through the taste-breaking artifacts: there is one would-be Goldstone boson, and 15 additional heavier "pions", which results in an RMS pion mass larger than the mass of the would-be Goldstone boson. This effect is depicted in Fig. 1 for different staggered type fermion actions. As can be seen for this figure, the previously used twice stout smeared action ("2stout") has a larger RMS pion mass and thus taste-breaking effects than the HISQ/tree action. If, however, the number of smearing steps is increased to four, with slightly smaller smearing strength ("4stout"), the RMS pion mass measured agrees with that of the HISQ/tree action. In order to have an improved pion sector, we, therefore, opted to switch to this new action and to restart our production runs.

So far, the equation of state is known only in 2+1 flavor QCD. Here, the status of the field is marked by our papers on the $N_f = 2 + 1$ equation of state [2, 3] (see Fig. 2). The contribution from the sea charm quarks most likely matter at least for $T > 300$–$400\,\text{MeV}$ (for an illustration, see Fig. 3).

1.1 Reference Point: The $N_f = 2 + 1$ Equation of State

In [3] we have presented the first full calculation of the $N_f = 2 + 1$ Equation of State (EoS) of Quantum Chromodynamics (QCD) (still using our 2stout action). This result is the reference point for our calculation of the charmed EoS, and already included one continuum extrapolated result at $T = 214\,\text{MeV}$ for the trace anomaly using our new lattice action including a dynamical charm quark ($N_f = 2 + 1 + 1$).

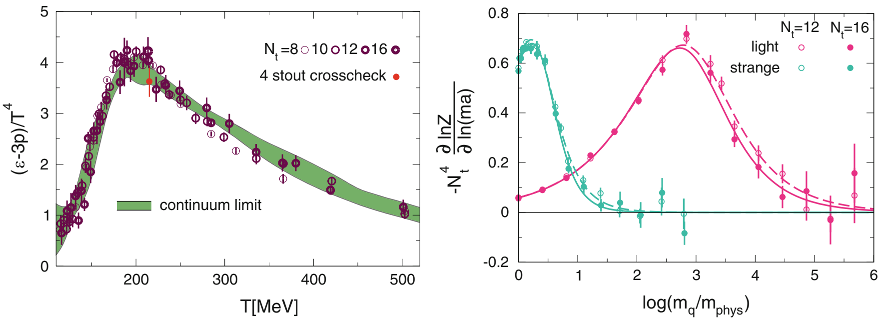

Fig. 2 *Left:*The trace anomaly as a function of the temperature. The continuum extrapolated result with total errors is given by the *shaded band*. Also shown is a cross-check point computed in the continuum limit with our new and different lattice action at $T = 214$ MeV, indicated by a *smaller filled red point*, which serves as a crosscheck on the peak's hight. *Right:* Setting the overall scale of the pressure: integration from the infinitely large mass region down to the physical point using a range of dedicated ensembles and time extents up to $N_t = 16$; the sum of the areas under the curves gives p/T^4. This result could be used for the cEoS normalization as well (see text)

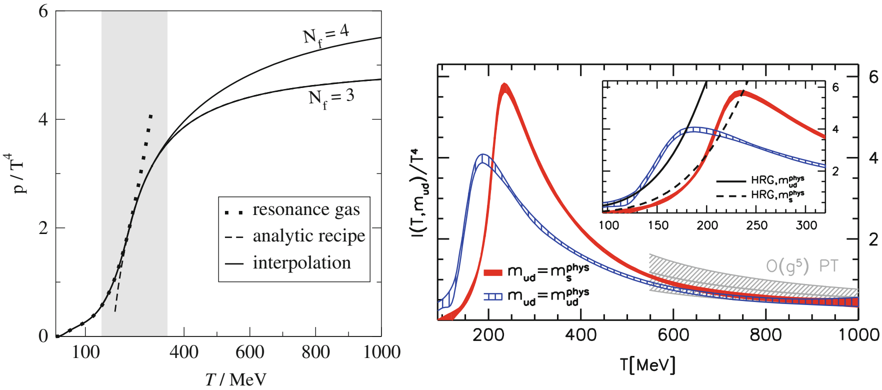

Fig. 3 *Left:* Laine and Schroeder's perturbative estimate of the effect of the charm in the QCD equation of state [4]. *Right:* Wuppertal-Budapest [2] and perturbative (up to $O(g^5)$) results for the equation of state

As visible in Fig. 2, at this temperature the charm quark is not yet relevant, since the $N_f = 2 + 1 + 1$ (continuum) data point falls right onto the (continuum) $N_f = 2 + 1$ curve. Below this temperature, we can compare the results with and without dynamical charm and can even use the $N_f = 2 + 1$ results to renormalize the $N_f = 2 + 1 + 1$ curve [5, 6].

2 Progress for the Charmed Equation of State

The $N_f = 2+1$ lattice results mentioned in the previous section agree with the HRG at low temperatures and are correct for the small to medium temperatures, and, as is shown in Fig. 3, at temperatures of about 1 GeV perturbative results become sufficiently precise. Therefore, we need to calculate the EoS with a dynamical charm only for the remaining temperatures in the region of approximately 300 MeV $< T <$ 1000 MeV.

We are using our 4stout lattice action for these calculations. The crosscheck point shown in Fig. 2 was computed using this new action. Since it perfectly agrees with the $N_f = 2+1$ results, even though it was computed using a dynamical charm, we can be certain that at temperatures at and below $T = 214$ MeV, we can rely on the $N_f = 2+1$ results.

Our preliminary results are shown in Fig. 4, all errors are statistical only. Our results span a region of temperatures from $T = 214$ MeV up to $T = 1.2$ GeV. At the low end we make contact to the $N_f = 2+1$ equation of state, and at large temperatures to the HTL result. Thereby, we cover the full region of temperatures, from low temperatures, where the HRG gives reliable results, to high temperatures, where we make contact with perturbation theory. The figure contains **new data points** at $N_t = 12$ generated in the last period.

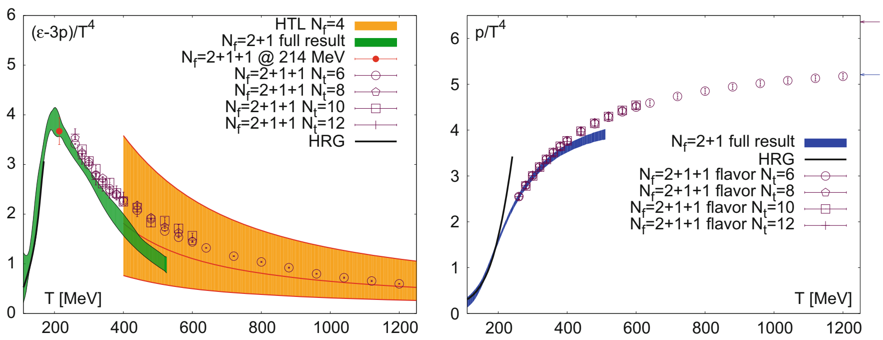

Fig. 4 *Left:* Preliminary results for the charmed EoS. For comparison, we show the HRG result, the $N_f = 2+1$ band, and, at high Temperatures, the HTL result [7], where the *central line* marks the HTL expectation for the EoS with the band resulting from (large) variations of the renormalization scale. *Right:* Preliminary result for the pressure, errors indicate the Stefan-Boltzmann value. All errors are statistical only

2.1 Line of Constant Physics

With the switch to a new lattice action comes the need to (re-) compute the LCP. In order to be able to reach large temperatures ($\beta > 4$), we have extended these calculations since the last report. Since we would like to span the temperature range from approximately 300 MeV $< T <$ 1000 MeV, we have to compute the LCP for a large range of couplings or lattice spacings. We split this range up in three overlapping regions (since we have to make sure that the derivative is smooth) according to the applicable simulation strategies.

At medium to coarse lattice spacings (region I) one can afford to use spectroscopy to tune the parameters. This is shown in Fig. 5. Here, we bracketed the physical point defined through M_π/f_π and $(2M_K - M_\pi)/f_\pi$ and, through interpolation, tune the light and strange quark masses to per-mill precision.

Using the parameters computed in this way, we then performed simulations on JUROPA at the SU(3) flavor-symmetrical point [8], extrapolating the results to our target couplings. There, we tuned the parameters to reproduce the extrapolated results. Since the quark masses are larger than physical, such simulations are considerably less costly than using spectroscopy as for region I, and we are thus able to compute a precise LCP down to fine lattice spacings of $a = 0.05$ fm (region II), where the HMC starts being affected by the freezing of topology (Fig. 6).

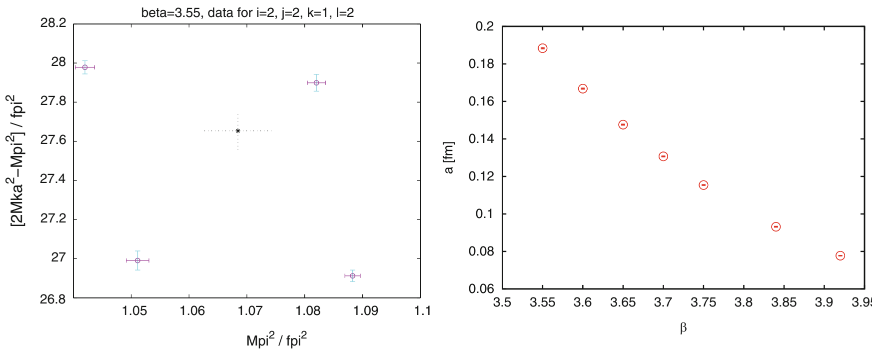

Fig. 5 Region of the LCP, for coarse to medium lattice spacing ($a > 0.08$ fm). Here, dedicated simulations bracketing the physical point archive a sub-percent accuracy for the LCP. *Left:* Bracketing of the physical point defined through M_π/f_π and $(2M_K - M_\pi)/f_\pi$. The strange quark mass is tuned (m_s/m_l is not fixed) and the ratio of the charm to strange quark mass is set at $m_c/m_s = 11.85$. *Right:* LCP computed through spectroscopy

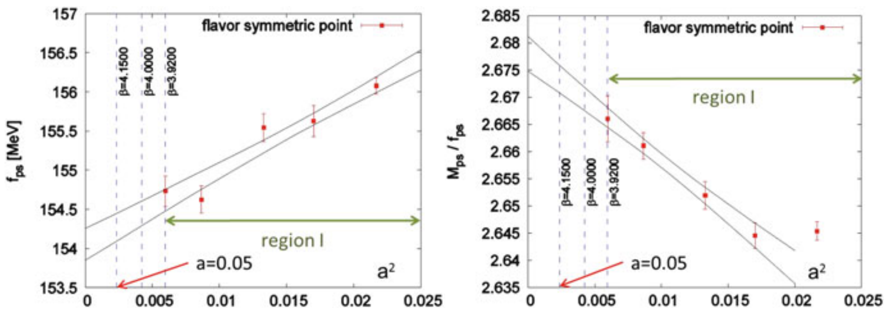

Fig. 6 Using the LCP computed from spectroscopy for coarse to medium lattice spacings (region I), dedicated simulations in the SU(3) flavor-symmetrical point [8] using these parameters are extrapolated towards the continuum. At the target coupling, the parameters are tuned until they reproduce the extrapolated value. In this way the LCP is extended to medium to small lattice spacings of $0.08 > a > 0.05$ fm (region II)

For finer lattice spacings we thus used our established step scaling procedure [3] based on the w_0 scale. To this end, we computed the observable

$$\mathcal{O} = t\frac{d}{dt}\left[t^2 E(t)\right]\Big|_{0.01L^2}$$

at three different lattice spacings (a_0, a_1, a_2) and volumes (16^4, 20^4, 24^4) chosen to keep the physical volume fixed, extrapolated to $a_3 = 24/32 a_2$, and tuned the coupling to match the extrapolated result. Using this method, we extended the LCP to very fine lattice spacings with $a < 0.05$ fm (region III).

2.2 *Additional Results*

In another effort, we calculated the neutron-proton and other mass splittings from first principles [9], using simulations of the combined theories of Quantum Electro- and Quantum Chromodynamics. Here, we used Hermit for valence calculations, i.e. we analyzed configurations generated elsewhere, computing the mass difference for a number of different bare parameters. The complete result is shown in Fig. 7. Due to the long range nature of Quantum Electrodynamics (QED) these simulations face significant finite-size effects, inducing shifts in the results considerably larger than the signal. Through analytical calculations (see SOM of [9]), we were able to predict and thus subtract these effects. Another important step was the development of a new update algorithm for the QED, which reduced the autocorrelation by more than 2 orders of magnitude.

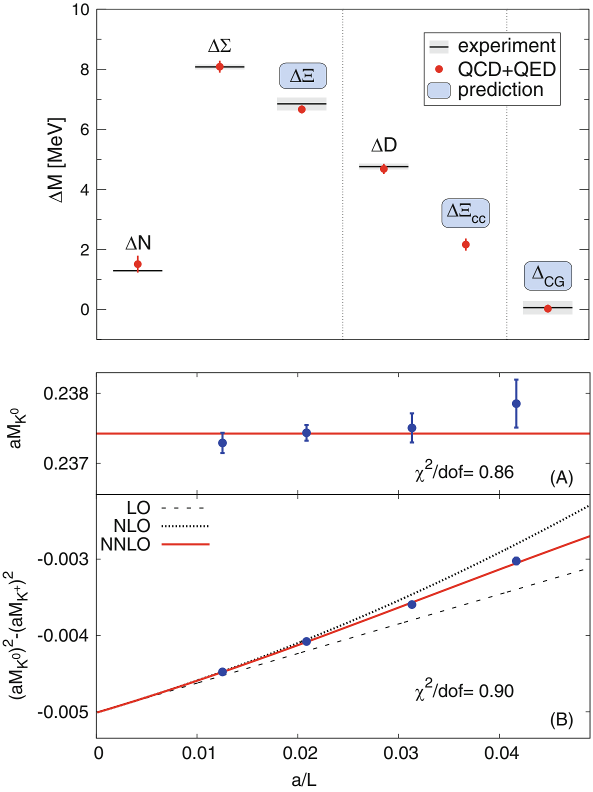

Fig. 7 *Left:* Mass splittings. The *horizontal lines* are the experimental values and the *grey shaded regions* represent the experimental error. Our results are shown by *red dots* with their uncertainties. Splittings which have either not been measured in experiment or are measured with less precision than in our calculation are indicated by a *blue shaded* region around the label. *Right:* Finite-volume behavior of kaon masses. (*A*) The neutral kaon mass, M_{K^0}, shows no significant finite volume dependence; L denotes the linear size of the system. (*B*) The mass-squared difference of the charged kaon mass, M_{K^+}, and M_{K^0} indicates that M_{K^+} is strongly dependent on volume. This finite-volume dependence is well described by an analytical results [9] (Figures taken from *Science* **347** 1452, reference [9]. Reprinted with permission from AAAS.)

3 Production Specifics and Performance

Most of our production is done using modest partition sizes, as we found these to be most efficient for our implementation.

3.1 Performance

Our code shows nice scaling properties on HERMIT and HORNET. For our scaling analysis below, we used two lattices ($N_s = 32$ and 48) and several partition sizes up to 256 nodes (HERMIT). We timed the most time consuming part of the code: the fermion matrix multiplication. The results are summarized in the following table:

No. of nodes	Gflop/node $N_s = 32$	Gflop/node $N_s = 48$
1	16.3	15.4
2	16.8	16.0
4	16.5	16.2
8	16.3	16.3
16	16.3	16.3
32	16.8	16.0
64	17.1	16.5
128	19.2	16.5
256	16.3	16.0

Test show that our scaling on HORNET is similarly good - however at a higher performance of $\approx$ 22 and $\approx$ 21 Gflop/s for the $N_s = 32$ and $N_s = 48$ lattices, respectively.

3.2 Production

Given the nice scaling properties of our code, we were able to run at the sweet spot for queue throughput, which we found to be located at a job size of 64 nodes. Larger job sizes proved to have a scheduling probability sufficiently low that benefits in the runtime due to the larger number of cores were compensated and the overall production throughput decreased. We, therefore, opted to stay at jobs sizes with 64 nodes.

4 Outlook

We believe we will be able to publish within the year. HERMIT and HORNET have proved to be essential tools enabling us to achieve this goal.

5 Publications of the Project

5.1 Peer-Reviewed

[9] *Ab initio calculation of the neutron-proton mass difference*, Science **347** (2015) 1452–1455

[10] *Equation of state, fluctuations and other recent results from LQCD*, Proceedings of the 30th Winter Workshop on Nuclear Dynamics (WWND 2014), J.Phys.Conf.Ser. **535** (2014) 012016

5.2 Other

[11] *From quarks to hadrons and back - spectral and bulk phenomena of strongly interacting matter*, Proceedings of the XXVI IUPAP Conference on Computational Physics (CCP2014), J. Phys. Conf. Ser. **640** (2015) 012053

[12] *Recent results on the Equation of State of QCD*, Proceedings of the 32nd International Symposium on Lattice Field Theory (Lattice 2014), PoS(**LATTICE2014)** 224

References

1. Borsanyi, S., Endrodi, G., Fodor, Z., Katz, S.D., Krieg, S., et al.: The QCD equation of state and the effects of the charm. PoS **LATTICE2011**, 201 (2011). [1204.0995]
2. Borsanyi, S., Endrodi, G., Fodor, Z., Jakovac, A., Katz, S.D., et al.: The QCD equation of state with dynamical quarks. J. High Energy Phys. **1011**, 077 (2010). [1007.2580]
3. Borsanyi, S., Fodor, Z., Hoelbling, C., Katz, S.D., Krieg, S., et al.: Full result for the QCD equation of state with 2+1 flavors Phys. Lett. **B730**, 99–104 (2014). [1309.5258]
4. Laine, M., Schroder, Y.: Quark mass thresholds in QCD thermodynamics. Phys. Rev. **D73** 085009 (2006). [hep-ph/0603048]
5. Endrodi, G., Fodor, Z., Katz, S., Szabo, K.: The equation of state at high temperatures from lattice QCD. PoS **LAT2007**, 228 (2007). [0710.4197]
6. Borsanyi, S., Endrodi, G., Fodor, Z., Katz, S., Szabo, K.: Precision SU(3) lattice thermodynamics for a large temperature range. J. High Energy Phys. **1207**, 056 (2012). [1204.6184]
7. Andersen, J.O., Leganger, L.E., Strickland, M., Su, N.: Three-loop HTL QCD thermodynamics. J. High Energy Phys. **1108**, 053 (2011). [1103.2528]
8. Bietenholz, W., Bornyakov, V., Gockeler, M., Horsley, R., Lockhart, W., et al.: Flavour blindness and patterns of flavour symmetry breaking in lattice simulations of up, down and strange quarks. Phys. Rev. **D84**, 054509 (2011). [1102.5300]
9. Borsanyi, S., Durr, S., Fodor, Z., Hoelbling, C., Katz, S., et al.: Ab initio calculation of the neutron-proton mass difference. Science **347**, 1452–1455 (2015). [1406.4088]

10. Wuppertal-Budapest Collaboration, Krieg, S.: Equation of state, fluctuations and other recent results from LQCD. In: Proceedings of the 30th Winter Workshop on Nuclear Dynamics (WWND 2014) (2014); J. Phys. Conf. Ser. **535**, 012016 (2014). doi:10.1088/1742-6596/535/1/012016
11. Budapest-Marseille-Wuppertal Collaboration, Wuppertal-Budapest Collaboration, Krieg, S.: From quarks to hadrons and back - spectral and bulk phenomena of strongly interacting matter. In: Proceedings of the 26th Conference on Computational Physics (CCP 2014) (2014); J. Phys. Conf. Ser. **640**(1), 012053 (2015). doi:10.1088/1742-6596/640/1/012053
12. Borsányi, S., Fodor, Z., Hoelbling, C., Katz, S.D., Krieg, S., Ratti, C., Szabo, K.K.: Recent results on the equation of state of QCD. In: Proceedings of the 32nd International Symposium on Lattice Field Theory (Lattice 2014) (2014); PoS **LATTICE2014**, 224 (2015) [arXiv:1410.7917]